ANALYSIS AND DESIGN P/C CYLINDRICAL SHELLS

by

WAIN-LAI KUO

Diploma, Taipei Institute of Technology, 1968

A MASTER'S REPORT

submitted in partial fulfillment of the

requirements for the degree

MASTER OF SCIENCE

Department of Civil Engineering

KANSAS STATE UNIVERSITY

Manhattan, Kansas

1976

Approved By:

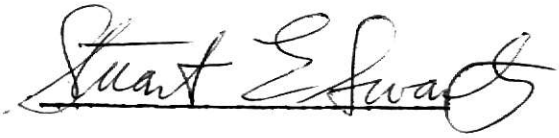

Major Professor

TABLE OF CONTENTS

	Page
LIST OF FIGURES	iii
LIST OF TABLES	V
I. INTRODUCTION AND SCOPE	1
II. LITERATURE SURVEY	2
III. METHOD OF ANALYSIS	5
1. SURFACE GEOMETRY	5
2. LOAD BALANCING METHOD	5
3. BEAM THEORY	5
4. MEMBRANE THEORY	8
5. THE BENDING THEORY	11
IV. NUMERICAL SOLUTIONS AND DESIGN EXAMPLE	19
1. COMPARISON BETWEEN BEAM THEORY SOLUTION AND BENDING THEORY SOLUTION FOR THE P/C SHELL WITHOUT EDGE BEAM UNDER DEAD LOAD, SNOW LOAD AND CABLE LOAD	19
2. DESIGN EXAMPLE	20
3. COMPARISON BETWEEN THE P/C CYLINDRICAL SHELL WITHOUT EDGE BEAM AND THE P/C CYLINDRICAL SHELL WITH EDGE BEAM	23
V. DISCUSSION AND CONCLUSIONS	25
REFERENCES	27
APPENDIX. - NOTATION	28
ACKNOWLEDGEMENTS	31
ABSTRACT	

LIST OF FIGURES

		Page
Figure 1.	Notation of Displacement and Forces	38
Figure 2.	Cylindrical Shell Prestressed for Load Balancing	38
Figure 3.	Longitudinal Stress and Transverse Shear Stress Distributions	39
Figure 4.	Longitudinal Stress and Transverse Shear Distributions with Prestressing Force Acting on the Shell . . .	39
Figure 5.	Properties of Arch Cross Section	39
Figure 6.	Component Loads	39
Figure 6.	(a) Dead Load	39
Figure 6.	(b) Snow Load	40
Figure 6.	(c) Prestressing Load	40
Figure 7.	Force Acting on the Arch	40
Figure 8.	Internal Tractions	41
Figure 9.	Principle of Load Transformation for Prestressing with a Curved Cable	42
Figure 10.	(a) The P/C Clyindrical Shell without Edge Beams	43
Figure 10.	(b) The P/C Clyindrical Shell with Edge Beams	43
Figure 11.	Shearing Forces and Transverse Moments in Shell without Edge Beams	44
Figure 12.	Longitudinal and Transverse Forces in Shell without Edge Beams	45
Figure 13.	Tangential Shearing Force $N_{x\phi}$ in Shell without Edge Beams	46
Figure 14.	Tangential Shearing Force $N_{x\phi}$ in Shell with Edge	

Page

Beam 46

Figure 15. Longitudinal and Transverse Forces in Shell with Edge Beams 47

Figure 16. Radial Shearing Forces and Transverse Moments in Shell with Edge Beams 48

Figure 17. Cables and Reinforcement Placement of P/C Shell without Edge Beams 49

Figure 18. Cables and Reinforcement Placement of P/C Shell without Edge Beams 50

Figure 19. Prestressing Cables in the Edge Beam of P/C Shell 51

Figure 20. Shell Section with Transverse Moment and Thrust 51

LIST OF TABLES

Page

TABLE 1. Comparison Between Beam Theory Solution and Bending Theory Solution for the Shell without Edge Beam 32

TABLE 2. Beam Theory Solution for the Shell without Edge Beam under Dead Load and Cable Load Only 33

TABLE 3. The Resultant Forces for the Shell with Edge Beam (Bending Theory) 34

TABLE 4. Comparison of Design Results for the Shell with Edge Beam and without Edge Beam 35

TABLE 5. Stresses in Edge Beam 35

TABLE 6. Bar Number and Spacing for Transverse Reinforcement for Shell without Edge Beam Corresponding to W_ϕ & M_ϕ at $x = 0$ 36

TABLE 7. Bar Number and Spacing for Transverse Reinforcement for Shell with Edge Beam Corresponding to N_ϕ & M_ϕ at $x = 0$ 36

TABLE 8. Bar Number and Spacing for Diagonal Reinforcement for Shell with Edge Beam Corresponding to Tp_1 at $\phi = 0°$ 37

I. INTRODUCTION AND SCOPE

The first concrete shell was built in Europe as early as 1924, but there was little or no interest in this form of construction in the United States, until 1954, when The First Conference on Thin Shells which met at MIT may be said to have marked a definite turning point. Since that time, engineers and architects have become increasingly aware of the economic and aesthetic possibilities offered by shell roofs for enclosing large column-free spaces required for a variety of applications.

As the span of a cylindrical shell becomes large, the tension in the shell edge or the edge beam reaches a very high value demanding the provision of very heavy reinforcement. Additionally, the deflections become excessive and large transverse moments are created which at the crown can not be readily resisted. For these reasons, a design in reinforced concrete often tends to be uneconomical. Prestressing the shell is the answer.

The purpose of this report is to compare the design of a prestressed cylindrical shell without edge beams with that for a prestressed cylindrical shell with edge beams. A description of the methods of analysis is presented and comparisons made between the two designs in terms of stress distributions. Cost considerations for the two designs are also made.

II. LITERATURE SURVEY

History of Design and Construction of Shells

The thin reinforced-concrete shell, as we know it today, had its beginnings in Germany in the 1920s. Most of the early shells built were cylindrical barrels. In 1924, the first concrete shell roof was designed by Carl Zeiss and built in the Zeiss works in Jena, Germany.

History of Analysis Methods (7, 9)

The first analytical approach to the design of shells was presented by G. Lame' and E. Clapeyron, who in 1826 produced the "membrane analogy" in which a shell was considered capable of resisting external loads by direct stresses unaccompanied by any bending. The next important contribution in this field was made in 1892 by A. E. H. Love, who developed mathematical conceptions which made possible a more accurate analysis than could be achieved by membrane analogy. Around the year 1923 U. Finsterwalder and F. Dischinger were the first to develop a theoretical analysis applicable to reinforced concrete cylindrical shells. In the United States, H. Schorer further simplified the derivation of Finsterwalder (1936). Until about 1940, the cylindrical shell more or less dominated the scene. The beam theory for shell analysis was developed by H. Lundgren of Denmark in 1949. This consists of seperate analyses in which the shell is considered first as a beam and secondly as an arch. The load balancing method, which was developed by T. Y. Lin, for prestressed concrete member offers a new approach and greatly simplifies the design of prestressed shells.

Design Consideration

(a) Selection of shell type (7). For covering very large areas, for hangars,

warehouses, etc., short shells are usually economical. The span of the short shell may be chosen as between one-sixth and one-third of the chord width. A practical limit on the span of long reinforced-concrete shells is about 100 ft. For longer shells, prestressing will prove economical.

(b) The radius of a cylindrical shell has (7) to be chosen keeping acoustic considerations in view. It is desirable to see that the center of curvature does not lie at the working level.

(c) Semicentral angle (7)

The practice is to keep the semicentral angle between 30°and 45°. If the angle exceeds 45°, concreting becomes difficult without the use of top forms. If the angle is below 40°, wind load can be ignored, because it causes only a suction on the shell.

(d) Thickness (7, 9)

The minimum thickness of reinforced-concrete cylindrical shells is governed by practical considerations such as acommodating reinforcement and providing adequate cover. According to a Dutch report (7) the usual recommended thickness is between 7 and 8 cm. A minimum of 4 cm is recommended by the Institute for Typification of the German Democratic Republic at Berlin

(e) Width of Edge Beam (7)

A width of two to three times the thickness of the shell would usually suffice. A minimum of 6" is demanded by practical considerations

(f) Design of Reinforcement (non-prestressed) (8)

a) The ratio of steel to concrete in any portion of the tensile zone should not be less than 0.35% of the cross sectional area of concrete.

b) The minimum temperature and shrinkage steel should not be less than 0.14% of the cross sectional area of concrete.

c) The maximum spacing of bars should not exceed 40 bar diameters nor five times the thickness of the shell.

III. METHOD OF ANALYSIS

1. Surface Geometry

The cylindrical shell with a circular directrix and radius R is shown along with the coordinate systen in Fig. 1 where the positive direction of the load components per unit area of the surface are also indicated.

2. Load Balancing Method

Consider the cylindrical shell without edge beams in Fig 2. The cables can be post-tensioned along the shell surface so that the vertical component of a cable will balance the gravity load. The prestressing forces, and its vertical component W_v and horizontal component W_h are given by (6)

$$H = \frac{W\ell^2}{8f_v} \frac{1}{2}, \qquad (3 - 1a)$$

$$W_v = H \frac{8f_v}{\ell^2}, \qquad (3 - 1b)$$

$$W_h = H \frac{8f_h}{\ell^2}. \qquad (3 - 1c)$$

In these expressions W is the uniform load of the shell per linear ft anlong the X axis, ℓ is the span of the shell, f_v is the projected vertical sag of the parabolic cable and f_h is the projected horizontal sag of the parabolic cable.

3. Beam Theory

The beam theory involves two analyses:

(A) The beam analysis (Fig. 3)

(i) The longitudinal stresses at any cross section of the shell are computed on the basis of the simple flexural theory

$$N_x = \frac{Mc}{I} \quad , \qquad (3 - 2a)$$

where I is the moment of inertia of the shell cross-section about the axis yy. (Fig. 5) It may be shown that (7)

$$I = R^3 t[\phi_c + \sin\phi_c(\cos\phi_c - \frac{2\sin\phi_c}{\phi_c})] \quad . \qquad (3 - 2b)$$

The shearing stresses are computed by the corresponding simple expression

$$N_{x\phi} = \frac{VQ}{Ib} \quad , \qquad (3 - 2c)$$

where Q is the first statical moment of the cross section up to the point under consideration about the axis yy and is (7)

$$Q = 2\ R^2 t\ (\sin\phi - \frac{\phi\sin\phi_c}{\phi_c}) \qquad (3 - 2d)$$

(ii) For the case of the prestressing force acting on the shell (Fig.4) the vertical component of the cable force is equal to some gravity load, therefore, the beam shear force and bending moment are zero for this load.

The longitudinal force is

$$N_x = -\frac{2H}{A} \quad , \qquad (3 - 3a)$$

where A is the cross-sectional area of the shell,

The following equations for transverse forces and moments have been developed by using the free bodies shown in Fig. 6. The force F_v was obtained by summing vertical forces, and M_ϕ by taking moments about the intersection of a radial line at angle ϕ and the arc of the shell.

a) Forces due to Dead Load (Fig. 6a)

$$F_v = gR\,(\phi_c - \phi), \qquad (3-4a)$$

$$M\phi = -gR^2[\cos\phi - \cos\phi_c - \sin\phi\,(\phi_c - \phi)], \qquad (3-4b)$$

$$N\phi = gR\,(\phi_c - \phi)\sin\phi, \qquad (3-4c)$$

$$Q\phi = -gR\,(\phi_c - \phi)\cos\phi. \qquad (3-4d)$$

b) Forces due to Snow Load (Fig. 6b)

$$F_v = p_o R\,(\sin\phi_c - \sin\phi), \qquad (3-5a)$$

$$M\phi = -\tfrac{1}{2}\,p_o R^2(\sin\phi_c - \sin\phi), \qquad (3-5b)$$

$$N\phi = p_o R\sin\phi(\sin\phi_c - \sin\phi)^2, \qquad (3-5c)$$

$$Q\phi = -p_o R\cos\phi(\sin\phi_c - \sin\phi). \qquad (3-5d)$$

c) Forces due to Prestressing Load (Fig. 6c)

$$M\phi = -W_{hi}R\,[\cos\phi - \cos\phi_i(\chi)] - W_{vi}R\,[\sin\phi - \sin\phi_i(\chi)], \qquad (3-6a)$$

$$N\phi = -W_{hi}\cos\phi - W_{vi}\sin\phi, \qquad (3-6b)$$

$$Q\phi = -W_{hi}\sin\phi + W_{vi}\cos\phi, \qquad (3-6c)$$

in which $M\phi = N\phi = Q\phi = 0$ when ϕ is greater than $\phi_i(\chi)$.

(B) The Arch Analysis

When forces acting on the shell are balanced by prestressing forces, there is no shear flow produced at all, which means no arch

action in the shell; but when the acting forces are unbalanced by the prestressing forces, shear flow will appear and the arch action will have an effect on the shell response. The vertical components of the shear flow balance the load on the shell arch; the horizontal components of the shear flow which are symmetrically disposed about the crown balance themselves. The resulting internal forces are

$$F_v = -\int_{\phi}^{\phi_c} \frac{gR^2\phi_c\, Q(\theta)}{I} \sin\phi d\theta + gR(\phi_c - \phi) \qquad (3 - 8a)$$

$$F_h = -\int_{\phi}^{\phi_c} \frac{gR\phi_c\, Q(\theta)}{I} \cos\phi R d\theta \qquad (3 - 8b)$$

$$Q\phi = - F_v \cos\phi + F_h \sin\phi \qquad (3 - 8c)$$

$$N\phi = F_v \sin\phi + F_h \cos\phi \qquad (3 - 8d)$$

$$M\phi = \int_{\phi}^{\phi_c} gR^3\phi_c Q(\theta) \sin\phi (\sin\theta - \sin\phi)\, d\theta - \int_{\phi}^{\phi_c} gR^3\phi_c Q(\theta) \cos\phi (\cos\phi - \cos\theta)\, d\theta - gR^2[\cos\phi - \cos\phi_c - \sin\phi (\phi_c - \phi)]. \qquad (3 - 8e)$$

4. Membrane Theory

The differential equations of equilibrium of a shell based on membrane theory are given by

$$\frac{\partial N_x}{\partial x} + \frac{1}{R} \frac{\partial N_{x\phi}}{\partial \phi} + X = 0 \qquad (3 - 9a)$$

$$\frac{1}{R}\frac{\partial N\phi}{\partial \phi} + \frac{\partial Nx\phi}{\partial x} + Y = 0 \ , \qquad (3 - 9b)$$

$$N\phi - RZ = 0 \ , \qquad (3 - 9c)$$

where the angle ϕ is measured from the crown.

Substituting stress-strain relations and strain-displacement relations into the equilibrium equations, and combining gives the resultant forces.

(1) Stresses and Displacements under Dead Load (7)

A uniform load g is developed in a Fourier Series as

$$g = \frac{4}{\pi} g \sum_{n=1,3,5,\ldots}^{\infty} \frac{(-1)^{\frac{n-1}{2}}}{n} \cos \frac{n\pi x}{L} \ . \qquad (3 - 10)$$

Taking only the first term into account, the components of the dead load are

$$x = 0, \qquad (3 - 11a)$$

$$Z = -\frac{4}{\pi} g \cos\frac{\pi x}{\ell} \cos\phi \ , \qquad (3 - 11b)$$

$$Y = -\frac{4}{\pi} g \cos\frac{\pi x}{\ell} \sin\phi \ , \qquad (3 - 11c)$$

Now from (3 - 9c),

$$N\phi = -\frac{4}{\pi} Rg \cos\frac{\pi x}{\ell} \cos\phi \ , \qquad (3 - 12a)$$

From (3 - 9b),

$$N_{x\phi} = -\int \left(\frac{1}{R}\frac{\partial N_\phi}{\partial \phi} + Y\right) dx = \frac{8\ell}{\pi^2} g \sin\frac{\pi x}{\ell} \sin\phi \ , \qquad (3 - 12b)$$

From (3 - 9a),

$$N_x = -\frac{1}{R}\int\frac{\partial N_{x\phi}}{\partial\phi}\,dx = -\frac{8g\ell^2}{R\pi^3}\cos\frac{\pi x}{\ell}\cos\phi\,, \qquad (3-12c)$$

The corresponding displacements can be shown to be the following:

(7)

Transverse displacement,

$$v = +\frac{8g}{\pi Et}\sin\phi\cos\frac{\pi x}{\ell}\left(\frac{2}{k^2}+\frac{1}{R^2k^4}\right), \qquad (3-12d)$$

where $k = \pi/\ell$, corresponding to the first Fourier term.

Normal displacement,

$$w = \frac{\partial v}{\partial\phi} = -\frac{8g}{\pi Et}\cos\phi\cos\frac{\pi x}{\ell}\left(\frac{2}{k^2}+\frac{1}{R^2k^4}\right), \qquad (3-12e)$$

Longitudinal displacement,

$$u = -\frac{1}{Et}\frac{8g}{\pi Rk^3}\cos\phi\ \sin\frac{\pi x}{\ell} \qquad (3-12f)$$

(ii) Stresses and Displacement under snow load (7)

As before, a snow load p_s can be represented as

$$p_o = \frac{4}{\pi} \sum_{n=1,3,5,..}^{\infty} \frac{(-1)^{\frac{n-1}{2}}}{n} \cos \frac{n\pi x}{\ell} \quad .$$

Proceeding in the same manner as for the dead load the following expressions will be obtained (7),

$$N\phi = -\frac{4}{\pi} p_o R \cos \frac{\pi x}{\ell} \cos^2 \phi \qquad (3 - 13a)$$

$$Nx\phi = -\frac{6}{\pi^2} p_o \ell \sin \frac{\pi x}{\ell} \sin 2\phi \qquad (3 - 13b)$$

$$Nx = -\frac{12}{R\pi^3} p_o \ell^2 \cos \frac{\pi x}{\ell} \cos 2\phi \qquad (3 - 13c)$$

$$v = +\frac{12}{Et\pi^5} p_o R^2 \left(\frac{\ell}{R}\right)^4 \left[\left(\frac{R\pi}{\ell}\right)^2 + 2\right] \sin 2\phi$$

$$\cos \frac{\pi x}{\ell} , \qquad (3 - 13d)$$

$$w = \frac{24}{Et\pi^5} p_o R^2 \left(\frac{\ell}{R}\right)^4 \left[\left(\frac{R\pi}{\ell}\right)^2 + 2\right] \cos 2\phi$$

$$\cos \frac{\pi x}{\ell} , \qquad (3 - 13e)$$

and

$$u = -\frac{12}{Et\pi^4 R} p_o \ell^3 \cos 2\phi \sin \frac{\pi x}{\ell} . \qquad (3 - 13f)$$

5. The Bending Theory

(A) The forces affecting the equilibrium of the shell element are set up by referring to Fig. 8.

$$\frac{\partial N_x}{\partial x} + \frac{1}{R}\frac{\partial N_{x\phi}}{\partial \phi} = 0, \qquad (3-14a)$$

$$\frac{\partial N_\phi}{\partial \phi} + R\frac{\partial N_{\phi x}}{\partial x} = 0, \qquad (3-14b)$$

$$R\frac{\partial Q_x}{\partial x} + \frac{\partial Q_\phi}{\partial \phi} + N_\phi = 0, \qquad (3-14c)$$

$$R\frac{\partial M_{x\phi}}{\partial x} + \frac{\partial M_\phi}{\partial \phi} - R\,Q_\phi = 0, \qquad (3-14d)$$

$$\frac{\partial M_{\phi x}}{\partial \phi} + R\frac{\partial M_x}{\partial x} - R\,Q_x = 0, \qquad (3-14e)$$

$$N_{x\phi} - N_{\phi x} = 0. \qquad (3-14f)$$

Substituting stress-strain relations and strain-displacement relations into the equilibrium equations, and combining leads to (1)

$$\left[R^8\frac{\partial^8}{\partial x^8} + 4R^6\frac{\partial^8}{\partial x^6\partial \phi^2} + 6R^4\frac{\partial^8}{\partial x^4\partial \phi^4} + 4R^2\frac{\partial^8}{\partial x^2\partial \phi^6} + \frac{\partial^8}{\partial \phi^8}\right]w + \frac{R^4}{\cancel{k}}\frac{\partial^4 w}{\partial x^4} = 0\,. \qquad (3-15)$$

This is Donnell's equation in w.

Use the following formulation for w which satisfies the boundary conditions at the ends, i.e.

$$w = He^{m\phi}\cos\frac{\lambda_n x}{R}\,, \qquad (3-16)$$

in which H = const, m = parameter, $\lambda_n = \frac{\pi R}{\ell}$.

Substituting this into Eq. (3 - 15) leads to

$$(m^2 - \lambda_n^2)^4 + \frac{\lambda_n^4}{\epsilon} = 0, \qquad (3 - 17)$$

where

$$\epsilon = t^2/(12\ R^2) .$$

The eight roots $m_1, m_2, \ldots . m_8$ of the solution of Eq. (3 - 17) are

$$m_1 = \alpha_1 + i\beta_1 \qquad m_5 = - m_1$$

$$m_2 = \alpha_1 - i\beta_1 \qquad m_6 = - m_2$$

$$m_3 = \alpha_2 + i\beta_2 \qquad m_7 = - m_3$$

$$m_4 = \alpha_2 - i\beta_2 \qquad m_8 = - m_4$$

where

$$\alpha_1 = \frac{\rho}{8^{\frac{1}{4}}} [\sqrt{(1 + \kappa\sqrt{2})^2 + 1} + (1 + \kappa\sqrt{2})]^{\frac{1}{2}},$$

$$\alpha_2 = \frac{\rho}{8^{\frac{1}{4}}} [\sqrt{(1 - \kappa\sqrt{2})^2 + 1} - (1 - \kappa\sqrt{2})]^{\frac{1}{2}},$$

$$\beta_1 = \frac{\rho}{8^{\frac{1}{4}}} [\sqrt{(1 + \kappa\sqrt{2})^2 + 1} - (1 + \kappa\sqrt{2})]^{\frac{1}{2}}, \qquad (3 - 18)$$

$$\beta_2 = \frac{\rho}{8^{\frac{1}{4}}} [\sqrt{(1 - \kappa\sqrt{2})^2 + 1} + (1 - \kappa\sqrt{2})]^{\frac{1}{2}},$$

in which

$$p = \frac{\rho}{4\sqrt{2}} = \left(\frac{3\pi^4\ 6}{t^2\ \ell^4} \right)^{\frac{1}{8}}, \quad \kappa = \left(\frac{2\pi^4\ 2}{3\ \ell^4} \right)^{\frac{1}{4}}.$$

THIS BOOK CONTAINS NUMEROUS PAGES WITH DIAGRAMS THAT ARE CROOKED COMPARED TO THE REST OF THE INFORMATION ON THE PAGE.

THIS IS AS RECEIVED FROM CUSTOMER.

From strain displacement relationships, stress-strain relationships and assuming Poisson's Ratio is zero, the force and moment displacement equations are obtained in the following matrix form.

$$\begin{bmatrix} N_x \\ M_\phi \\ N_\phi \\ u \\ w \end{bmatrix} = \begin{bmatrix} \frac{4DRk^4}{p^2\kappa^2}\cos\frac{\pi x}{\ell} & 0 & 0 & 0 & 0 \\ 0 & \frac{2D}{R^2}\cos\frac{\pi x}{\ell} & 0 & 0 & 0 \\ 0 & 0 & \frac{-4DRk^4}{\kappa^2}\cos\frac{\pi x}{\ell} & 0 & 0 \\ 0 & 0 & 0 & \frac{4DRk^4}{E\kappa^3 t}\sin\frac{\pi x}{\ell} & 0 \\ 0 & 0 & 0 & 0 & 2 \end{bmatrix} x$$

$$\begin{bmatrix} -1 & 1+\kappa & 1 & 1-\kappa & 0 \\ 1+\kappa & 1 & \kappa-1 & 1 & 0 \\ 0 & 1 & 0 & -1 & 0 \\ -1 & 1+\kappa & 1 & 1-\kappa & 0 \\ 1 & 0 & 1 & 0 & 0 \end{bmatrix} \begin{bmatrix} f_1 & -f_2 & 0 & 0 & 0 \\ -f_2 & f_3 & 0 & 0 & 0 \\ 0 & 0 & f_3 & -f_4 & 0 \\ 0 & 0 & -f_4 & f_3 & 0 \\ 0 & 0 & 0 & 0 & 0 \end{bmatrix} \begin{bmatrix} A_n \\ B_n \\ C_n \\ D_n \\ 0 \end{bmatrix}$$

(3 - 19)

$$\begin{bmatrix} N_x \\ Q'_\phi \\ Q_\phi \\ v \\ \theta \end{bmatrix} = \begin{bmatrix} \frac{4DRk^4}{(\sqrt{\kappa})^5 p}\sin\frac{\pi x}{\ell} & 0 & 0 & 0 & 0 \\ 0 & \frac{2Dk^3}{(\sqrt{\kappa})^3 p}\cos\frac{\pi x}{\ell} & 0 & 0 & 0 \\ 0 & 0 & \frac{2Dk^3}{(\sqrt{\kappa})^3 p}\cos\frac{\pi x}{\ell} & 0 & 0 \\ 0 & 0 & 0 & \frac{4DRk^3}{E(\sqrt{\kappa})^7 tp}\cos\frac{\pi x}{\ell} & 0 \\ 0 & 0 & 0 & 0 & \cos\frac{\pi x}{\ell} \end{bmatrix} x$$

$$\begin{bmatrix} \beta_1 & \alpha_1 & \beta_2 & \alpha_2 & 0 \\ \alpha_1(1-\kappa)-\beta_1 & \alpha_1+\beta_1(1-\kappa) & -\alpha_2(1-\kappa)-\beta_2 & \alpha_2-\beta_2(1+\kappa) & 0 \\ \alpha_1-\beta_1 & \alpha_1+\beta_1 & \alpha_2+\beta_2 & \alpha_2-\beta_2 & 0 \\ \alpha_1+\beta_1(1-\kappa) & \beta_1-\alpha_1(1-\kappa) & -\alpha_2+\beta_2(1+\kappa) & -\beta_2-\alpha_2(1+\kappa) & 0 \\ \frac{2\alpha_1}{R}+\frac{(\bar{R}B_1)v}{R} & \frac{2\beta_1}{R}+\frac{(\bar{R}B_2)v}{R} & \frac{2\alpha_2}{R}+\frac{(\bar{R}-B_3)v}{R} & \frac{2\beta_2}{R}+\frac{(\bar{R}B_4)v}{R} & 0 \end{bmatrix} x$$

$$\begin{bmatrix} f'_1 & -f'_2 & 0 & 0 & 0 \\ -f'_2 & f'_1 & 0 & 0 & 0 \\ 0 & 0 & f'_3 & f'_4 & 0 \\ 0 & 0 & -f'_4 & -f'_3 & 0 \\ 0 & 0 & 0 & 0 & 0 \end{bmatrix} \begin{bmatrix} A_n \\ B_n \\ C_n \\ D_n \\ 0 \end{bmatrix}, \qquad (3-20)$$

Observe that one part of the coefficients B_1, etc., for θ are obtained from v, that is, $(\bar{R}B_1)v/R = \frac{4Dk^3}{Et(\sqrt{\kappa})^7 p}[\alpha_1+\beta_1(1-\kappa)]$.

in which $D = EI$, $f_1 = \cos\beta_1\phi \cosh\alpha_1\phi$, $f_2 = \sin\beta_1\phi \sinh\alpha_1\phi$,

$f_3 = \cos\beta_2\phi \cosh\alpha_2\phi$, $f_4 = \sin\beta_2\phi \sinh\alpha_2\phi$, $f_1' = \cos\beta_1\phi \sinh\alpha_1\phi$.

$f_2' = \sin\beta_1\phi \cosh\alpha_1\phi$, $f_3' = \cos\beta_2\phi \sinh\alpha_2\phi$, $f_4' = \sin\beta_2\phi \cosh\alpha_2\phi$,

the arbitrary constants A_n, B_n, C_n, and D_n.

(B) Formulation of boundary conditions for a P/C shell with edge beam

The boundary conditions applicable to this shell at its junction with the edge beam are stated as follows:

(a) The resultant horizontal force at shell edge is equal to zero, i.e.,

$$(N_\phi)_{m+b} \cos\phi_c - (Q_\phi')_b \sin\phi_c = 0 \qquad (3 - 21a)$$

(b) The transverse moment $M\phi$ at the shell edge is equal to zero, i.e., (assuming negligble torsion stiffness in the edge beam)

$$M\phi = 0 \qquad (3 - 21b)$$

(c) The vertical deflection of the shell edge is equal to the vertical deflection of the edge beam. This condition is formulated below.

1. The edge beam prestressed by a curved cable is shown in Fig. (9a). The effect of prestressing can be subdivided into three particular cases of loading (Fig. 9b): (4)

   (i) An upward vertical force W_v caused by the curvature of the cable,

$$W_V = \frac{8\,H(e + e_1)}{\ell^2} \,, \qquad (3\text{-}21c\text{-}1)$$

(ii) End moments M due to eccentricity of anchorage,

$$M = He_1 . \qquad (3\text{-}21c\text{-}2)$$

(iii) An axial compressive force H applied at both ends at the center of gravity of beam section.

For vertical displacement,

$$-(v)_{m+b} \sin\phi_c + (w)_{m+b} \cos\phi_c = \frac{1}{K^4EI}[(N\phi)_{m+b} \sin\phi_c + Q'_\phi \cos\phi_c - (N_{x\phi})_{m+b} ka_1 - \frac{4}{\pi} W + \frac{4}{\pi} \times \frac{8H(e+e_1)}{\ell^2} - \frac{4}{\pi} He_1k^2] \,. \qquad (3\text{-}21c\text{-}3)$$

2. Maximum stresses in edge beam

Shear force,

$$S_1 = \frac{1}{K}(Q_\phi \cos\phi_c + N_\phi \sin\phi_c - \frac{4}{\pi} W) \,; \qquad (3\text{-}21c\text{-}4)$$

$$\sigma_t = -\frac{H'}{A} + \frac{H(e+e_1)a_1}{I} - \frac{Ma_1}{I} \,; \qquad (3\text{-}21c\text{-}5)$$

$$\sigma_b = -\frac{H'}{A} - \frac{H(e+e_1)a_1}{I} + \frac{Ma_1}{I} \,; \qquad (3\text{-}21c\text{-}6)$$

$H' = H - F$ (tensile force due to shear at top of beam)

where a_1 is at top or bottom edge.

(d) Longitudinal displacement of the shell edge is equal to the longitudinal displacement of the edge beam at its juction with the shell, i.e.,

$$(u)_{m+b} = \{[(N_\phi)_{m+b} \sin\phi_c + (Q'_\phi)_{m+b}\cos\phi_c]a_1\frac{1}{k^4EI}\, k -$$

$$[(\frac{N_{x\phi}}{k^2})_{m+b}\frac{1}{AE}] - [(N_{x\phi})_{m+b}\, a_1{}^2k^2\frac{1}{k^4EI}] -$$

$$a_1\frac{1}{k^4EI}\, k\, \frac{4}{\pi}\, W\} . \qquad (3\text{-}21d)$$

IV. NUMERICAL SOLUTIONS AND DESIGN EXAMPLE

The P/C cylindrical shells without and with edge beam used for design examples are shown in Fig. 10.

Design Loads

Dead load g = 25 psf of surface area

Snow load p = 20 psf of horizontal projection

Maximum design load of Freyssinet System's cable=54,000 lb/cable

Material Parameters

Young's modulus $E = 360 \times 10^6$ psf

Poisson's ratio $\nu = 0$

1. Comparison between beam theory solution and bending theory solution for the P/C shell without edge beam under dead load, snow load and cable load. The results of computer calculations for the force resultants and the comparison between beam theory solution and bending theory solutions in which it is assumed that horizontal cable forces are acting on the shell edge are given Table 1. The results of beam solutions for dead load and cable load only are also shown in Table 2. Figs. 11, 12, and 13 illustrate the distribution of the force resultants.

   Comments on comparison of these results.

   (a) The values of N_ϕ show little difference at the crown between the two theories, but at the edge they are different.

   (b) The values of $N_{x\phi}$ are different. There is nothing in the beam solution because the gravity load is balanced by upward cable forces.

   (c) The compressive forces N_x, are constant at all cross sections in the beam solutions because there are no beam bending moments produced.

   (d) The transverse bending moment M_ϕ in the bending solutions are about 8

to 14 times of that in the beam solutions at midspan.

Generally, using a beam theory it is easier to analyze effects of the prestressing cables than using a bending theory in which it is assumed all the horizontal forces are acting on the shell edge.

2. Design Example for the shell without edge beam and the shell with edge beam (1, 8, 9)

(1) Reinforcement (using elastic method)

f_s = 24,000 psi, f_y = 60,000 psi, f_c = 1,800 psi,

f_c' = 4,000 psi

The minimum reinforcement ratio in the tensile zone at any portion should not less than 0.0035.

$A_s = 0.0035\ (12\ t)\ in^2/ft$

for t = 3 in, $A_s = 0.126\ in^2/ft$

Also, the maximum spacing of bars in any portion should not exceed 40 diameters or five times the thichness of the shell given in CRSI Design Handbook. In this design, this is 10".

(a) Longitudinal Steel for N_x

The requirement of steel area can be calculated by the following formula.

$$A_{s\ell} = \frac{N_x}{f_s}\ ,\ \text{if } N_x \text{ is in tension}$$

In the examples, the values of N_x are compressive at all cross sections, therefore, the bar number and the spacings are chosen based on the minimum temperature and shrinkage steel requirements.

(b) Diagonal Steel for the in-plane Shear Force

As can be observed from Figs. 13 and 14, the maximum shear force

for both shells $N_{x\phi}$ is at the end. Also note that shearing stresses in the shell without edge beam are low enough such that diagonal reinforcement is not necessary.

From determining the steel necessary to resist the tensile forces, the principal forces obtained by combining direct forces and tangential shears must be evaluated. This can be done by using the governing equations that

$$Tp = \frac{Nx + N\phi}{2} \pm \sqrt{(\frac{Nx - N\phi}{2})^2 + N_{x\phi}^2}$$

in which

T_p = the principal forces. The plane on which the first principal force acts is given by

$$\tan 2\bar{\theta} = \frac{2N_{x\phi}}{N_x - N\phi}$$

in which, for positive values of tan $2\bar{\theta}$, $\bar{\theta}$ is measured in a counter clockwise direction from the face on which N_x acts. With these, the steel cross sectional area as for the principal tensile forces can be calculated by the following equation,

$$A_{sd} = \frac{T_p}{f_s \cos^2(45°-\bar{\theta})}$$

For this, bar numbers and spacings for the shell with edge beams are given in Table 8.

(c) Transverse Steel for N_ϕ, M_ϕ

Figs. 11b, 12b, 15b, and 16b indicate that the maximum effects for N_ϕ, M_ϕ are in the midspan at the crown. For the shell without edge beam N_ϕ = -1,319 lb/ft, M_ϕ = -1,408 lb-ft/ft, and for

the shell with edge beam $N_\phi = -1{,}447$ lb/ft, $M_\phi = 815$ lb-ft/ft.

Observing Figs. 20a and 20b, the transverse reinforcement A_s for the maximum effect for N_ϕ, M_ϕ is calculated as follows.

For the P/C shell without edge beam the eccentricity

$$e = \frac{N_\phi jd + M_\phi}{N_\phi} = 13.68 \text{ in},$$

$$A_{st} = \frac{N_\phi(e - jd)}{f_s jd} = \frac{1{,}319(13.68 - 0.875 \times 2.625)}{24{,}000 \times 0.875 \times 2.625}$$

$$= 0.2724 \text{ in}^2/\text{ft},$$

the spacing and bar number are shown in Table 6.

For the P/C shell with edge beam the eccentricity

$$e = \frac{N_\phi jd + M_\phi}{N_\phi} = 7.63 \text{ in},$$

$$A_{st} = \frac{N_\phi(e - jd)}{f_s jd} = \frac{1{,}447(7.633 - 0.875 \times 2.625)}{24{,}000 \times 0.875 \times 2.625}$$

$$= 0.13 \text{ in}^2/\text{ft},$$

Results giving bar spacings and number are given for both shells in Tables 6 and 7.

(d) Tensile Steel for Edge Beams

$$A_s = \frac{\frac{1}{2} f_t B x}{f_s} = \frac{\frac{1}{2} \times 260 \times 6}{24{,}000} = 0.6165 \text{ in}^2$$

For this, bar numbers shown in Fig. 19.

(2) The adequacy of the design with respect to ACI 318-71 requirements

(a) The maximum steel area/per foot should be less than

$$\frac{7.2\ t\ f'_c}{f_y} = \frac{7.2 \times 3 \times 4{,}000}{60{,}000} = 1.44 \text{ in}^2,$$

or $$\frac{29{,}000\ t}{f_y} = \frac{29{,}000 \times 3}{60{,}000} = 1.45 \text{ in}^2 \qquad \text{O.K.}$$

(b) The maximum spacing

Because $4\phi\sqrt{f'_c}$ = 227.68 psi > the computed tensile stresses due to design load, the maximum spacing allowed could be greater than three times the thickness, 3h = 9, but not farther apart than five times the thickness nor 18 in. (capacity-reduction factor ϕ = 0.9)

(c) The ratio of the minimum reinforcement per foot to the concrete area is equal to 0.0014.

For #3 @15", A_s/ft = 0.088 in^2/ft, and

$$\frac{\text{steel area}}{\text{concrete area}} = \frac{0.088}{12 \times 3} = 0.00244 > 0.0014 \qquad \text{O.K.}$$

(d) The minimum reinforcement ratio in the tensile zone at any portion shall not be less than 0.0035

For #3 @10", A_s/ft = 0.13 in^2/ft

$$\frac{0.13}{12 \times 3} = 0.0036 > 0.0035 \qquad \text{O.K.}$$

3. Comparison between the P/C cylindrical shell without edge beam and the P/C cylindrical shell with edge beam.

The numerical solutions of the P/C shell without edge beam are based on beam theory, and the P/C shell with edge beam are based on the bending theory.

The comparisons of design results for these two shells are presented in Table 4. The results of the calculations for the force resultants of the P/C shell with edge beam are given in Table 3. Figs. 14, 15 and 16 illus-

strate the distribution of the force resultants. The stress resultants of the edge beam which are based on Eqs. (3-21c-4), (3-21c-5), and (3-21c-6) are also given in Table 5.

Comments on comparison of results.

(a) It is obvious that by the introduction of edge beam the shell as a unit has reduced forces and moments.

(b) The design results show that the P/C shell without edge beam requires more cables but less concrete; the P/C shell with edge beam needs more concrete and reinforcement but less cables.

4. Discuss the results shown in Figs. 17, 18 and 19.

The requirement of cables in the P/C shell without edge beam is twice that of the P/C shell with edge beam. The volume of concrete in the P/C shell without edge beam is about 40% less than that required in the P/C shell with edge beam, but the weight of steel used is almost the same for both cases.

Theoretically, there is no stirrup reinforcement required for the edge beam; usually some stirrup reinforcement are used to hold the cables in a stable position.

V, DISCUSSION AND CONCLUSIONS

1. The beam theory is easy and simple to use and also can be applied to shells with noncircular directrices.

2. The structural action of the shell using the beam theory is easily visualized.

3. In the bending solutions the force calculation are based upon only the first term of the Fourier Series.

4. The wind load was not taken into consideration in this report because the semicentral angle does not exceed 45°, and therefore the wind causes only a suction on the shell. This will result in a decrease in shell forces.

5. For the P/C shell with edge beam, the bending forces and longitudinal forces are small compared to those forces in the P/C shell without edge beam under dead load, snow load, and cable load.

6. It is much easier to layout the cables on the edge beam than those along the shell surface.

7. It has been shown that the P/C shell without edge beams needs more cables and reinforcement but less concrete, than the P/C shell with edge beam.

8. For design purposes the shell forces should be calculated under the action of dead load, snow load and cable load acting on the shell and dead load plus cable load only.

9. In order to eliminate cracks and reduce moments and deflections, prestress-

ing is often used in the long shell with edge beams. In this manner the difficulty in placing a great quantity of tension bars in the beams is avoided.

REFERENCES

1. Gibson, J. E., "The Design of Cylindrical Shell Roofs", 2nd ed., D. Van Nostrand Company Inc., New York 1954. (Reprinted 1961)

2. Billington, D. P., "Thin Shell Concrete Structures", McGraw-Hill Inc., N. Y. 1965.

3. Yitzhaki, D., "The Design of Prismatic and Cylindrical Shell Roofs", Haifa Offset, 1958, p. 111 - 116.

4. Dabrowski, R., "Analysis of Prestressed Cylindrical Shell Roofs", Journal of the structural Division, ASCE, vol. 89, No. s75, Proc. Paper 3668, October, 1963.

5. Chinn, James, "Cylindrical Shell Analysis Simplified by Beam Method", Journal of the American Concrete Institute, vol. 55, May, 1959, p. 1183.

6. Lin, T. Y., "Design of Prestressed Concrete Structures 2nd ed., John Wiley & Sons, Inc., N. Y., 1963, p. 339 - 369.

7. Ramaswamy, G. S. "Design and Construction of Concrete Shell Roofs", McGraw-Hill Inc., N. Y. 1968.

8. "Building Code Requirement for Reinforced Concrete (ACI 318 - 71)", American Concrete Institute, 1971. (1974 revision)

9. "Design of Cylindrical Concrete Shell Roofs: Manuals of Engineering Practice - No. 31", ASCE, New York, N. Y. 1952. (Reprinted 1956 and 1960)

APPENDIX. – NOTATION

The following symbols are used in this report:

A = cross-sectional area;

A_n = arbitrary constant;

A_s, A_{sd}, $A_{s\ell}$, A_{st} = the reinforcement steel cross-sectional area;

a_1 = height of edge beam;

B = width of beam;

B_1, B_2, B_3, B_4 = numerical coefficient;

B_n = arbitrary constant;

b = thickness of section, bending theory;

C_n = arbitrary constrants;

c = distance;

D = flexural rigidity, $D = Et^3/12(1-\nu^2)$

D_n = arbitrary constant;

e, e_1 = eccentricities of prestressing force with respect to the neutral axis of the beam;

E = Young's modulus;

F = tensile force;

F_v, F_h = vertical and horizontal reaction forces;

f_v, f_h = vertical and horizontal sag of cables;

f_1, f_2, f_3, f_4

f_5, f_6, f_7, f_8 = exponential terms;

f_c = compressive working strength of concrete, $0.45\ f'_c$;

f'_c = compressive strength of concrete;

f_s = working strength of steel, $0.4\ f_y$;

f_y = ultimate strength of steel;

g = gravity load per unit area of the surface;

H = prestressing force;

I = moment of inertia;

k = π/ℓ;

ℓ = longitudinal span;

M = bending moment;

M_ϕ = transverse moment, considered positive when it produces tension in the outward fibers;

$M_{x\phi}$ = twisting moment, considered positive when it produces tension in the outward fibers;

$m_1, m_2, m_3, m_4,$

m_5, m_6, m_7, m_8 = the eight roots of Donnell's equation;

N_ϕ = direct force component in the transverse direction, considered positive when tensile;

$N_{x\phi}$ = tangential shearing force, considered positive when tensile;

N_x = direct force component in the longitudinal direction, considered positive when tensile;

n = no terms of fourier's series;

p = constant;

p_o = snow load per unit area of the horizontal projection;

Q = first moment about neutral axis of area of cross section;

Q_ϕ = radial shearing force, considered positive when outward direction;

Q'_ϕ = combining the radial shearing force and the twisting moment, $Q'_\phi = Q_\phi + \partial M_{x\phi}/\partial x$;

$\bar{R}$ = numerical coefficient, $\bar{R} = \frac{4DRk^3}{E(\sqrt{\kappa})^7 tp}$;

R = radius of shell;

S_1 = shearing force;

T_p = principal force;

t = thickness of shell;

V = shear contributed by gravity load;

W = weight;

W_{hi} = horizontal prestressing force at ith cable;

W_{vi} = vertical prestressing force at ith cable;

X, Y, Z = the forces per unit area acting on the shell in the longitudinal, tangential, and radial directions;

x, y, z = coordinats of shell;

$\alpha_1, \alpha_2, \beta_1, \beta_2$ = numerical coefficient;

ν = Poisson's ratio;

u = longitudinal displacement of the shell, considered positive in the direction of increasing values of x;

v = tangential displacement of the shell, considered positive in the direction of increasing values of ϕ;

w = radial displacement of the shell, considered positive in the toward direction;

θ = rotation of the shell, considered positive when the section rotates counterclockwise;

ϕ = angle measured from the crown;

$\phi_i(x)$ = angle of th cable as the fountion of x;

ϕ_c = semicentral angle;

λ_n = $\pi R/\ell$;

σ_t = fiber stresses on the top of edge beam;

σ_b = fiber stresses on the bottom of edge beam;

ACKNOWLEDGEMENTS

The writer is indebted to his major adviser, Dr. Stuart E. Swartz, for invaluable advice and guidance during his study at Kansas State University and preparation of this report.

He is also grateful to Dr. Kuo-Kwang Hu for his encouragement and comments.

Genuine thanks are also extend to Dr. Hugh S. Walker for serving on the advisory committee and reviewing the manuscript.

Special appreciation is also expressed to his wife for her understanding and encouragements and for her patience and carefulness in typing this report.

Table 1. Comparison Between Beam Theory Solution and Bending Theory Solution for the Shell without Edge Beam

	Beam Theory Solution						Bending Theory Solution				
x	(degree)	N_x (lb/ft)	N_ϕ (lb/ft)	Q_ϕ (lb/ft)	M_ϕ (lb-ft/ft)	$N_{x\phi}$ (lb/ft)	N_x (lb/ft)	N_ϕ (lb/ft)	Q_ϕ (lb/ft)	M_ϕ (lb-ft/ft)	$N_{x\phi}$ (lb/ft)
0	0	-26,299	-1,319	0	-1,408	0	-16,837	-1,675	0	-8,521	0
	5	-26,299	-1,324	- 10	-1,406	0	-16,388	-1,663	- 138	-8,383	0
	10	-26,299	-1,334	- 29	-1,365	0	-15,048	-1,629	- 275	-7,970	0
	15	-26,299	-1,352	- 51	-1,278	0	-12,805	-1,575	- 409	-7,285	0
	20	-26,299	-1,375	- 78	-1,138	0	- 9,643	-1,567	- 538	-6,334	0
	25	-26,299	-1,403	-112	- 931	0	- 5,540	-1,433	- 663	-5,126	0
	30	-26,299	-1,435	-153	- 643	0	- 470	-1,362	- 783	-3,666	0
	35	-26,299	-1,469	-203	- 256	0	5,600	-1,308	- 901	-1,957	0
	40	-26,299	0	0	0	0	12,711	-1,286	-1,017	0	0
ℓ/4	0	-26,299	-1,319	0	-1,180	0	-11,903	-1,185	0	-6,026	0
	5	-26,299	-1,323	- 10	-1,178	0	-11,588	-1,176	- 98	-5,928	- 304
	10	-26,299	-1,334	- 29	-1,136	0	-10,640	-1,151	- 194	-5,635	- 581
	15	-26,299	-1,352	- 51	-1,050	0	- 9,054	-1,114	- 289	-5,151	- 801
	20	-26,299	-1,376	- 78	- 910	0	- 6,818	-1,066	- 381	-4,479	- 937
	25	-26,299	-1,403	-112	- 703	0	- 3,917	-1,013	- 469	-3,625	- 957
	30	-26,299	-1,435	-153	- 415	0	333	- 963	- 554	-2,592	- 831
	35	-26,299	- 466	- 94	- 90	0	3,960	- 925	- 637	-1,384	- 524
	40	-26,299	0	0	0	0	8,988	- 910	- 719	0	0
ℓ/2	0	-26,299	-1,319	0	-1,408	0	0	0	0	0	0
	5	-26,299	-1,324	- 10	-1,406	0	0	0	0	0	- 430
	10	-26,299	-1,335	- 29	-1,365	0	0	0	0	0	- 821
	15	-26,299	-1,352	- 51	-1,278	0	0	0	0	0	-1,133
	20	-26,299	-1,011	-126	-1,100	0	0	0	0	0	-1,324
	25	-26,299	- 257	-195	- 726	0	0	0	0	0	-1,354
	30	-26,299	90	-156	- 326	0	0	0	0	0	-1,175
	35	-26,299	51	- 73	- 78	0	0	0	0	0	- 741
	40	-26,299	0	0	0	0	0	0	0	0	0

Table 2. Beam Theory Solution for the Shell without Edge Beam Under Dead Load and Cable Load Only

x	ϕ (degree)	N_x (lb/ft)	N_ϕ (lb/ft)	Q_ϕ (lb/ft)	M_ϕ (lb-ft/ft)	$N_{x\phi}$ (lb/ft)
0	0	- 3,132	-2,143	0	-601	0
	5	- 4,245	-2,120	18	-630	0
	10	- 7,572	-2,052	22	-675	0
	15	-13,090	-1,947	16	-720	0
	20	-20,756	-1,819	- 5	-735	0
	25	-30,511	-1,685	- 45	-684	0
	30	-42,292	-1,569	-102	-527	0
	35	-55,980	-1,497	-176	-226	0
	40	-71,499	0	0	0	0
$\ell/4$	0	- 8,924	-2,143	0	-373	0
	5	- 9,757	-2,120	8	-401	- 397
	10	-12,254	-2,052	22	-447	- 757
	15	-16,392	-1,948	16	-492	-1,039
	20	-22,142	-1,819	- 5	-507	-1,206
	25	-29,457	-1,685	- 45	-455	-1,220
	30	-38,286	-1,568	-102	-299	-1,047
	35	-48,559	- 494	- 67	- 61	- 651
	40	-60,199	0	0	0	0
$\ell/2$	0	-26,299	-2,143	0	-601	0
	5	-26,299	-2,120	18	-630	- 796
	10	-26,299	-2,052	22	-675	-1,514
	15	-26,299	-1,930	16	-720	-2,078
	20	-26,299	-1,455	- 52	-698	-2,411
	25	-26,299	- 538	-128	-479	-2,440
	30	-26,299	- 44	-105	-211	-2,093
	35	-26,299	23	- 46	- 48	-1,302
	40	-26,299	0	0	0	0

Table 3. The resultant Forces For the Shell with Edge Beam (Bending Theory)

	Dead Load, Snow Load & Cable Load						Dead Load & Cable Load				
x	ϕ (degree)	N_x (lb/ft)	N_ϕ (lb/ft)	Q_ϕ (lb/ft)	M_ϕ (lb-ft/ft)	$N_{x\phi}$ (lb/ft)	N_x (lb/ft)	N_ϕ (lb/ft)	Q_ϕ (lb/ft)	M_ϕ (lb-ft/ft)	$N_{x\phi}$ (lb/ft)
0	0	-21,516	-1,447	0	815	0	-11,265	-807	0	467	0
	5	-20,953	-1,420	2	819	0	-11,022	-793	1	469	0
	10	-19,306	-1,342	0.5	826	0	-10,320	-752	0.8	474	0
	15	-16,710	-1,216	- 7	826	0	- 9,231	-687	- 3	476	0
	20	-13,389	-1,050	- 24	803	0	- 7,879	-599	- 13	464	0
	25	- 9,656	- 853	- 51	735	0	- 6,439	-493	- 28	427	0
	30	- 5,917	- 636	- 90	597	0	- 5,136	-374	- 52	349	0
	35	- 2,659	- 408	-142	361	0	- 4,243	-244	- 82	213	0
	40	- 441	- 179	-206	0	0	- 4,071	-106	-122	0	0
$\ell/4$	0	-15,214	-1,023	0	576	0	- 7,965	-571	0	330	0
	5	-14,816	-1,004	1	579	- 433	- 7,994	-561	0.9	332	- 434
	10	-13,652	- 949	0.4	584	- 849	- 7,297	-532	0.6	335	- 849
	15	-11,816	- 860	- 5	584	-1,229	- 6,527	-485	- 2	336	-1,229
	20	- 9,467	- 742	- 17	568	-1,561	- 5,571	-423	- 9	328	-1,561
	25	- 6,828	- 603	- 36	520	-1,839	- 4,553	-349	- 20	302	-1,839
	30	- 4,184	- 450	- 64	422	-2,062	- 3,632	-264	- 36	247	-2,062
	35	- 1,881	- 289	-100	255	-2,242	- 3,000	-173	- 58	150	-2,242
	40	- 312	- 127	-146	0	-2,400	- 2,879	- 75	- 86	0	-2,400
$\ell/2$	0	0	0	0	0	0	0	0	0	0	0
	5	0	0	0	0	- 613	0	0	0	0	- 613
	10	0	0	0	0	-1,200	0	0	0	0	-1,200
	15	0	0	0	0	-1,738	0	0	0	0	-1,738
	20	0	0	0	0	-2,208	0	0	0	0	-2,208
	25	0	0	0	0	-2,600	0	0	0	0	-2,600
	30	0	0	0	0	-2,916	0	0	0	0	-2,916
	35	0	0	0	0	-3,171	0	0	0	0	-3,171
	40	0	0	0	0	-3,395	0	0	0	0	-3,395

Table 4. Comparisons of Design Results for the Shell with Edge Beam and without Edge Beam

Item / Shell	No. of Cables	Volume of Concrete, ft^3	Weight of Steel, lb
P/C shell without edge beam	20	1,090	5,148
P/C shell with edge beam	10	1,840	5,210

Table 5. Stress in Edge Beam

Acting Load / Stress	Dead Load, Snow Load & Cable Load	Dead Load & Cable Load
Top fiber stress of edge beam	+ 33 psi	+260 psi
Bottom fiber stress of edge beam	-378 psi	-987 psi

Table 6. Bar Number and Spacing for Transverse Reinforcement for Shell without Edge Beam Corresponding to N_ϕ & M_ϕ at x=0

Region	y (ft)	Corresponding N_ϕ (lb/ft)	Corresponding M_ϕ (lb-ft/ft)	As in^2/ft	Bar No.	Spacing (in) c.c.
	0	-1,319	-1,408			
1				0.29	3	4½
	4,363	-1,334	-1,365			
2				0.29	3	4½
	8,726	-1,375	-1,138			
3				0.22	3	6
	13.089	-1,435	- 643			
4				0.22	3	6
	17.452	0	0			

Table 7. Bar Number and Spacing for Transverse Reinforcement for Shell with Edge Beam Corresponding to N_ϕ & M_ϕ at x=0

Region	y (ft)	Corresponding N_ϕ (lb/ft)	Corresponding M_ϕ (lb-ft/ft)	As (in^2/ft)	Bar No.	Spacing (in) c.c.
	0	-1,447	815			
1				0.13	3	10
	4.363	-1,341	826			
2				0.13	3	10
	8.726	-1,049	803			
3				0.11	3	12
	13.089	- 635	597			
4				0.11	3	12
	17.452	- 179	0			

1 kg = 2.2046 lb
1 in = 2.54 cm

Table 8. Bar Number and Spacing for Diagonal Reinforcement for Shell with Edge Beam Corresponding to Tp_1 at $\phi = 40°$

Region	x (ft)	Corresponding Tp_1 (lb/ft)	(in^2/ft)	Bar No.	(in) c.c.
	0	- 179			
1					
	15.625	- 241			
2			0.13	3	10
	23.4375	1,674			
3			0.13	3	10
	39.0625	3,668			
4			0.19	3	7
	46.875	4,085			
5			0.24	3	5½
	62.5	5,466			

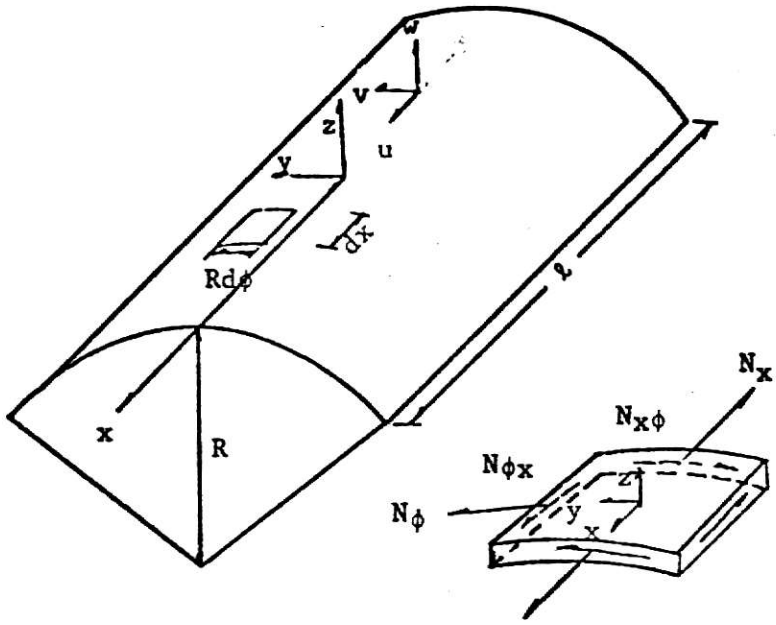

Fig. 1 Notation of Displacements and Forces

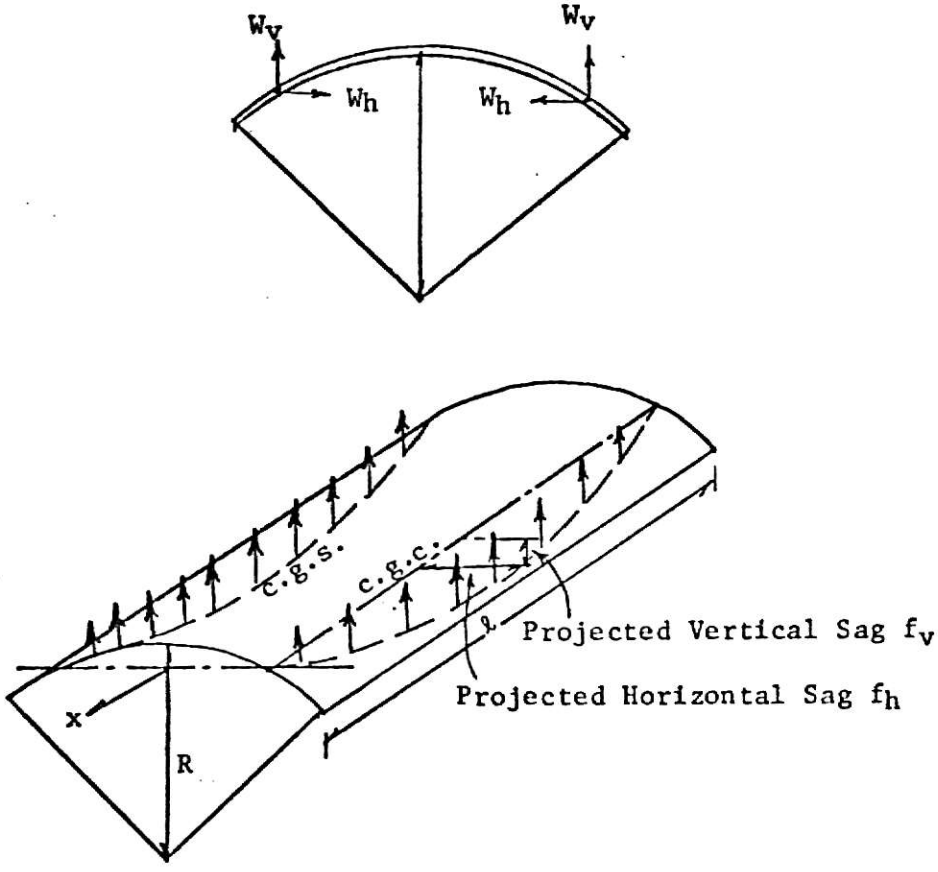

Fig. 2 Cylindrical Shell Prestressed for Load Balancing

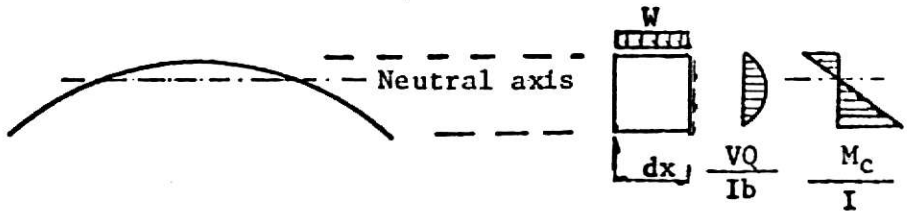

Fig. 3 Longitudinal Stress and Transverse Shear Stress Distributions

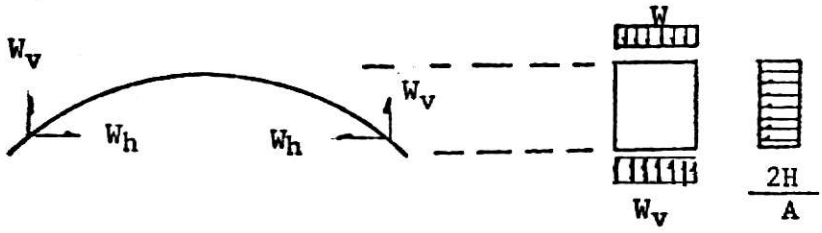

Fig. 4 Longitudinal Stress and Transverse Shear Distributions with Prestressing Force Acting on the Shell

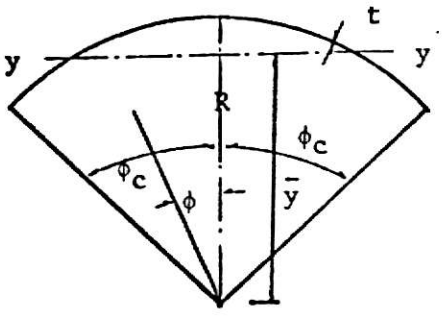

Fig. 5 Properties of Arch Cross Section

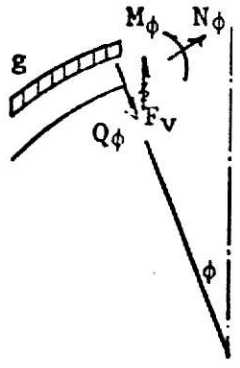

(a) Dead Load

Fig. 6 Component Loads

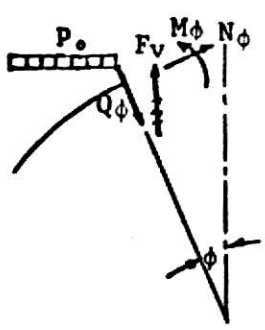

(b) Snow Load

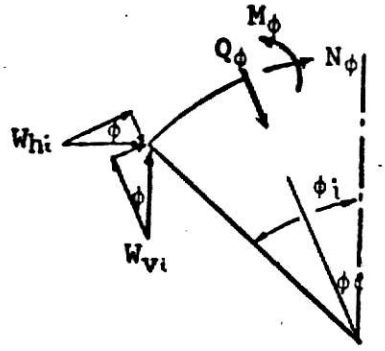

(c) Prestressing Load

Fig. 6 Component Loads

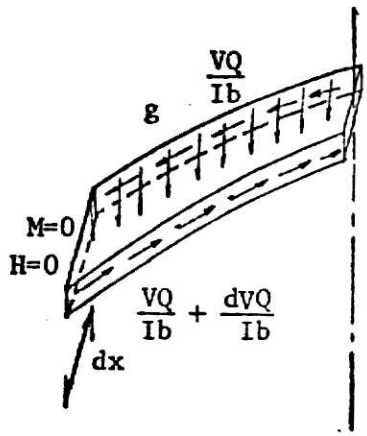

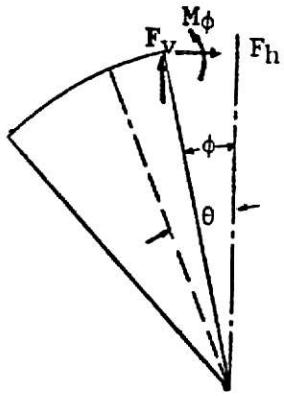

Fig. 7 Force Acting on the Arch

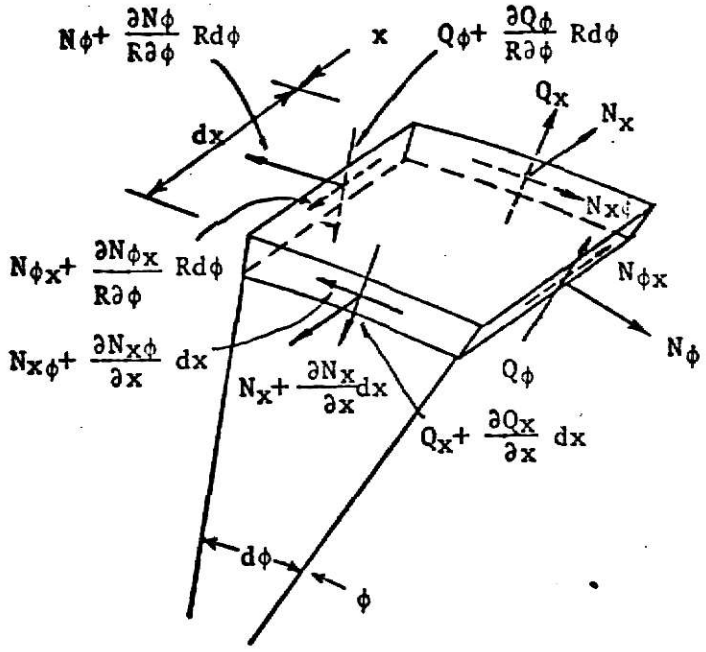

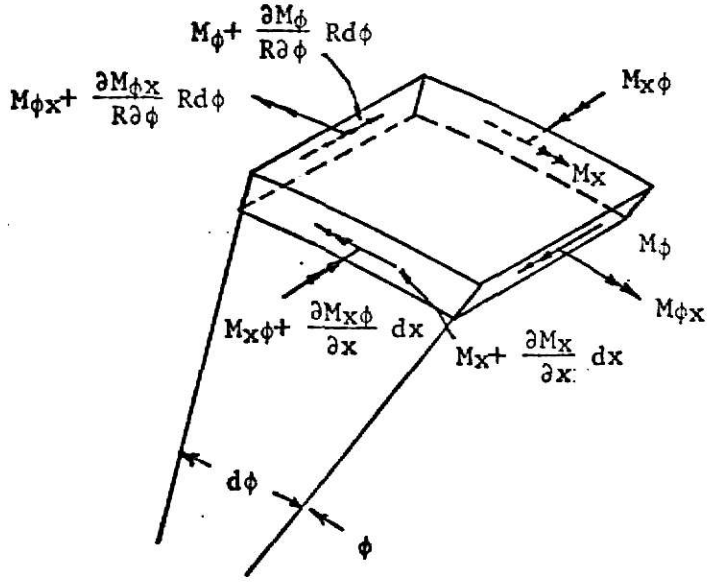

Fig. 8 Internal Tractions

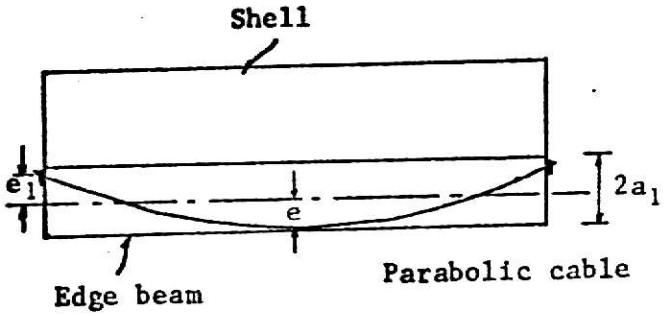

(a)

Case 1.

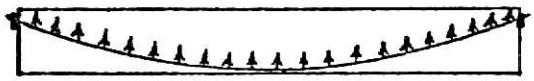

Uniform vertical load W_v

Case 2.

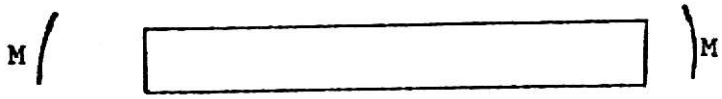

Case 3.

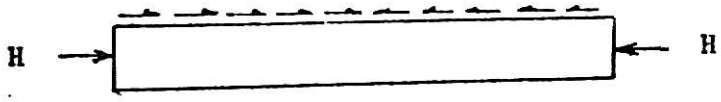

(b)

Fig. 9 Principle of Load Transformation for Prestressing with a Curved Cable

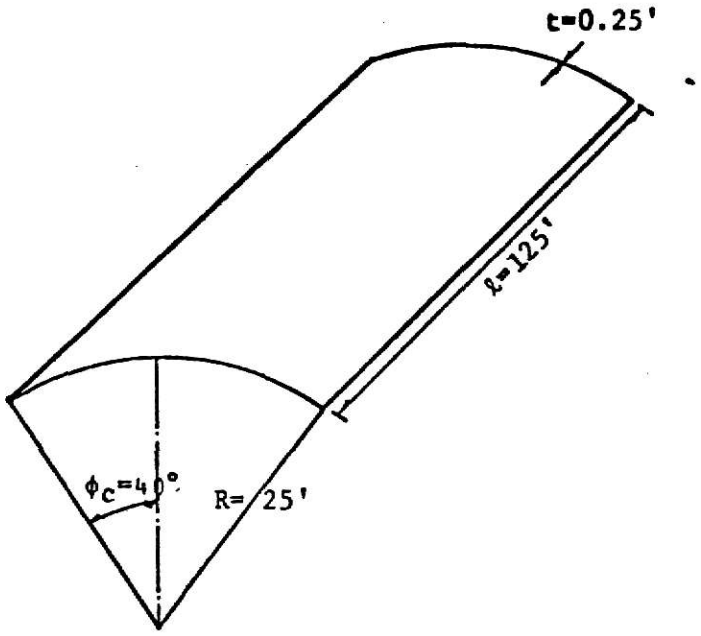

(a) The P/C Clyindrical Shell without Edge Beam

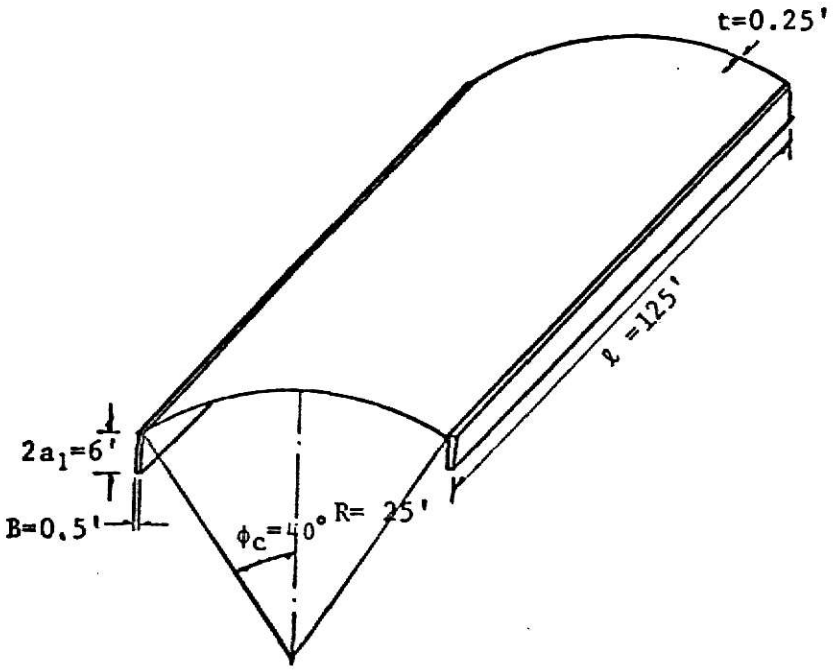

(b) The P/C Clyindrical Shell with Edge Beam

Fig. 10

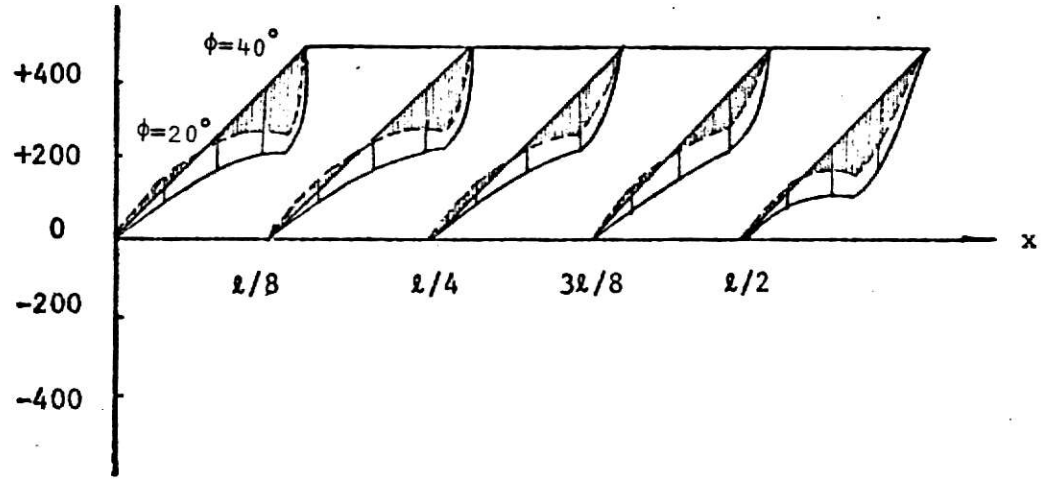

(a) Radial Shearing Force Q_ϕ (lb/ft)

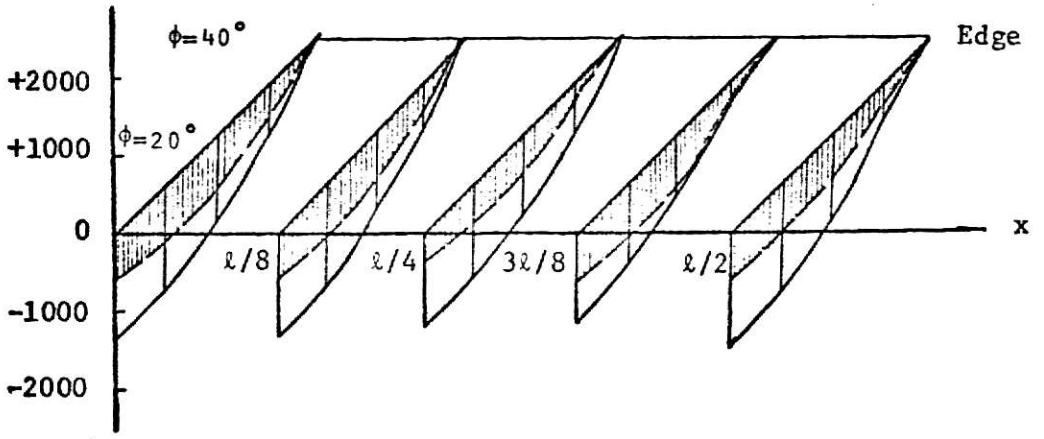

(b) Transverse Moment M_ϕ (lb-ft/ft)

Fig. 11 Shearing Forces and Transverse Moments in Shell without Edge Beam

——— Dead load + snow load + cable load

– – – – Dead load + cable load

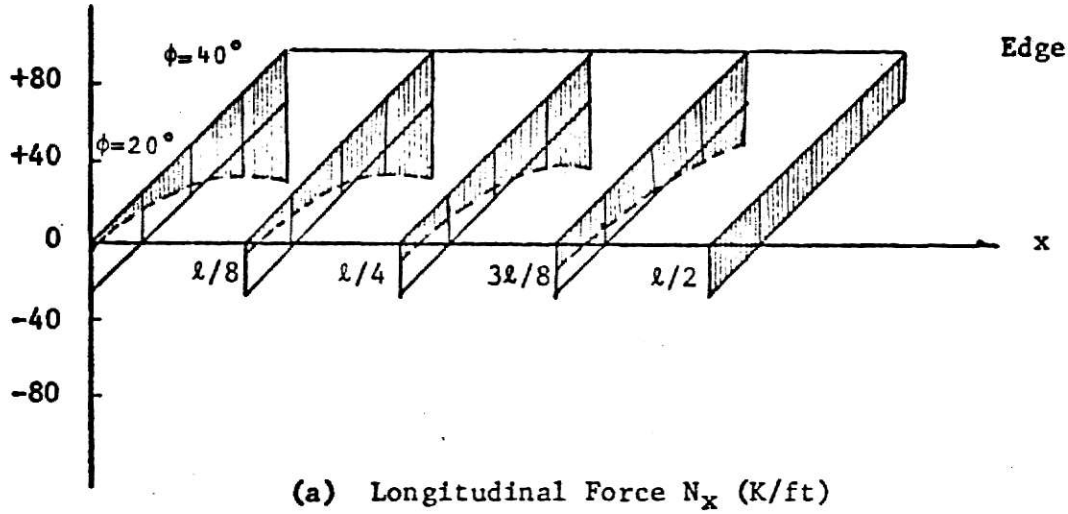

(a) Longitudinal Force N_x (K/ft)

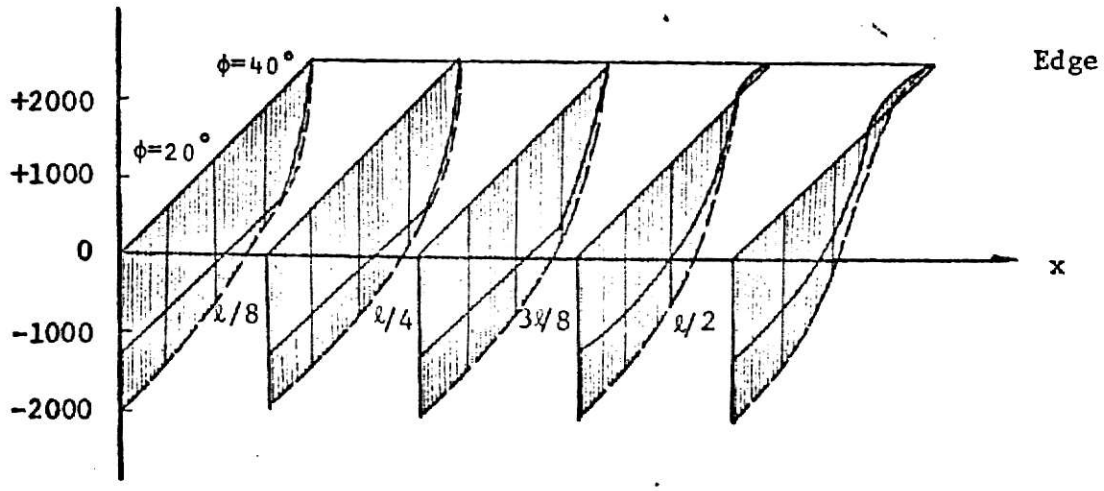

(b) Transverse Force N_ϕ (lb/ft)

Fig. 12 Longitudinal and Transverse Forces in Shell without Edge Beam

——— Dead load + snow load + cable load

– – – – Dead load + cable load

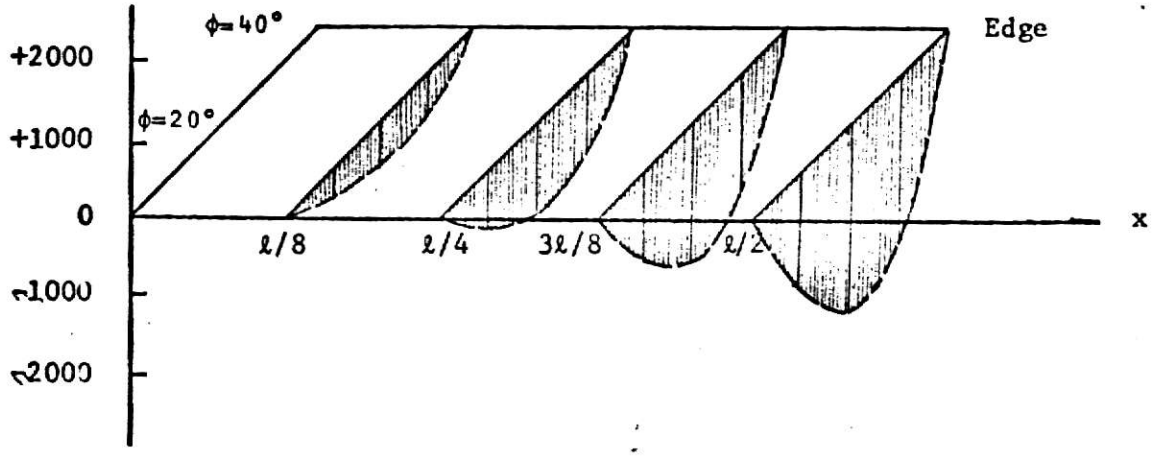

Fig. 13 Tangential Shearing Force $N_{x\phi}$(lb/ft)

in Shell without Edge Beam

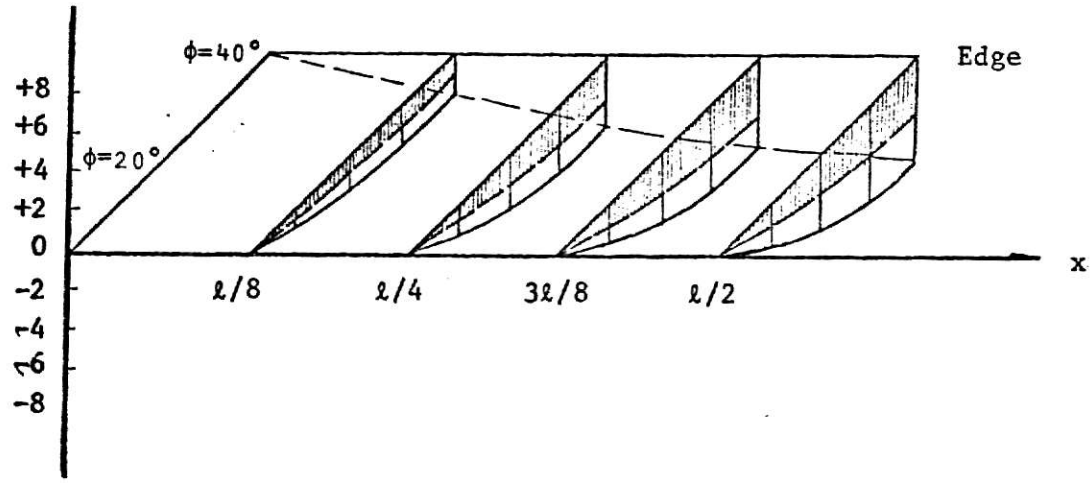

Fig. 14 Tangential Shearing Force $N_{x\phi}$(K/ft)

in Shell with Edge Beam

——— Dead load + snow load + cable load

— — — Dead load + cable load

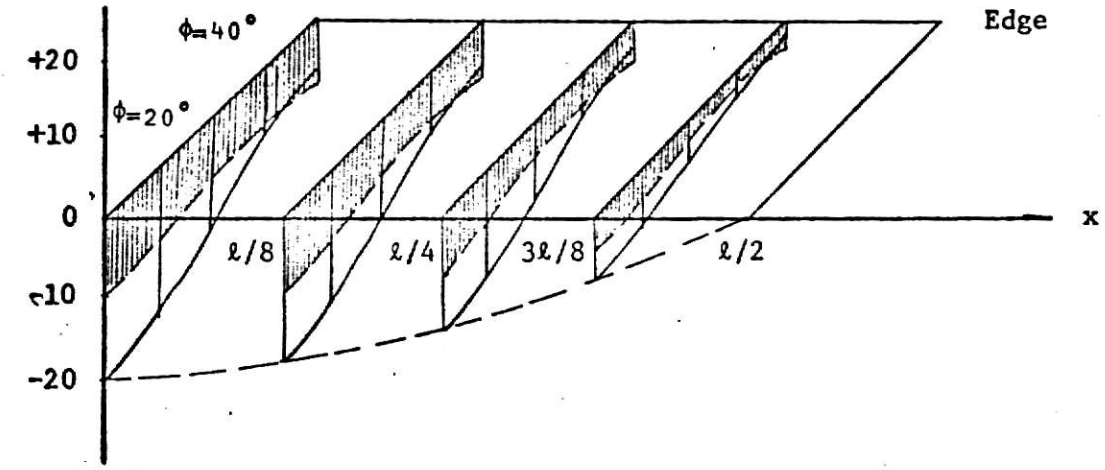

(a) Longitudinal Force N_x(K/ft)

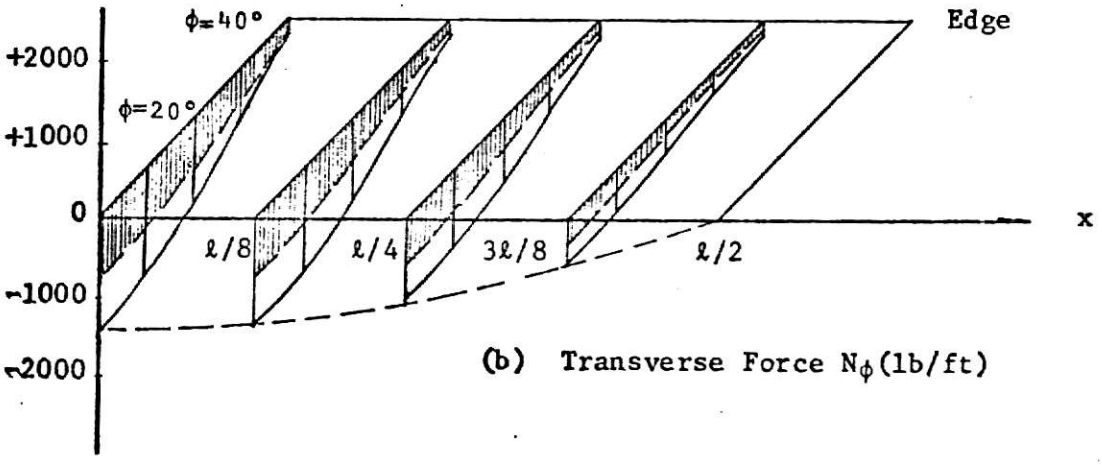

(b) Transverse Force N_ϕ(lb/ft)

Fig. 15 Longitudinal and Transverse Forces in Shell with Edge Beam

——— Dead load + snow load + cable load

– – – – Dead load + cable load

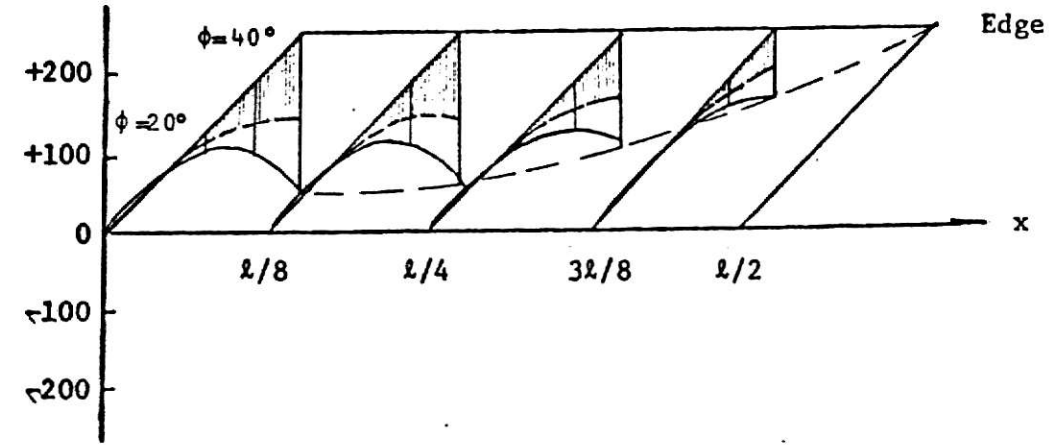

(a) Radial Shearing Force Q_ϕ(lb/ft)

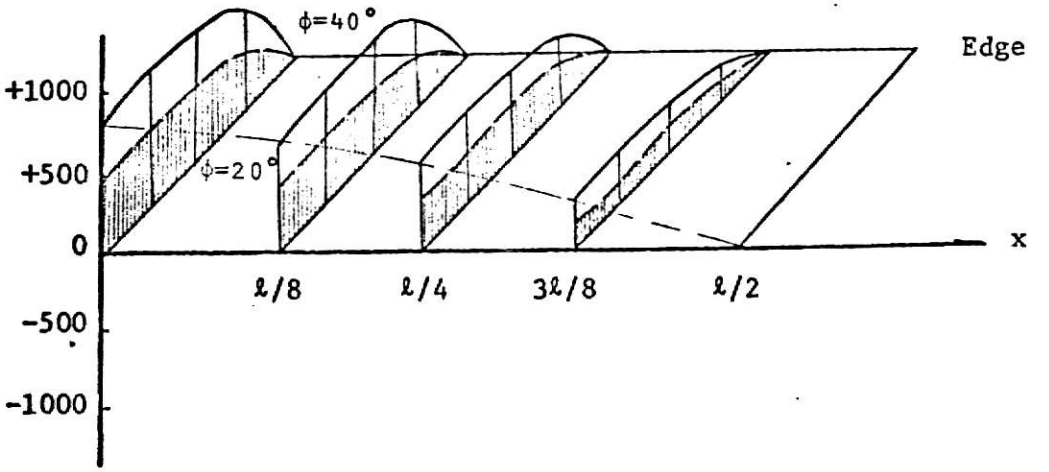

(b) Transverse Moment M_ϕ(lb-ft/ft)

Fig. 16 Radial Shearing Forces and Transverse Moments in Shell with Edge Beam

——— Dead load + snow load + cable load

– – – – Dead load + cable load

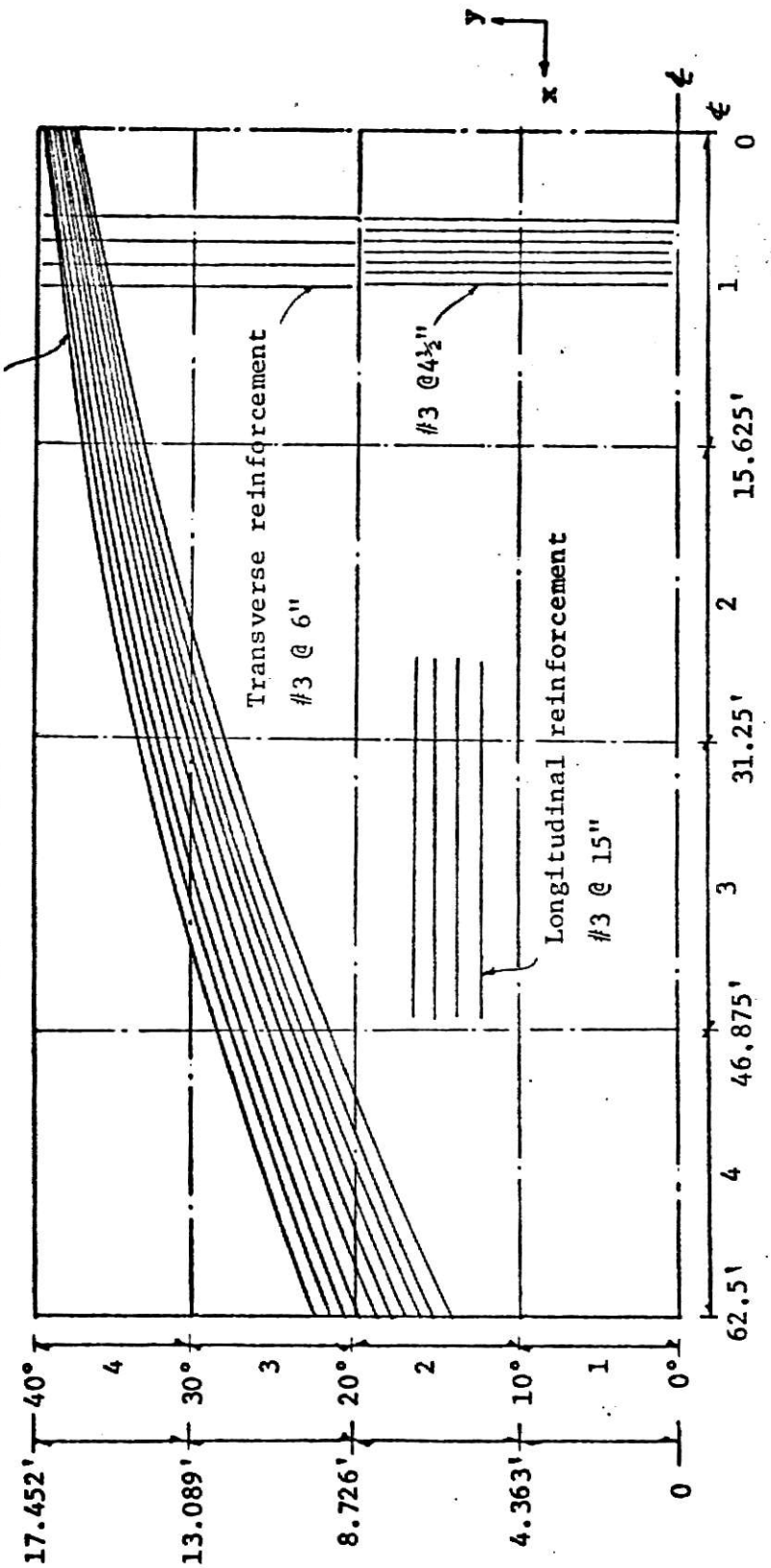

Fig. 17 Cables and Reinforcement Placement of P/C Shell without Edge Beams

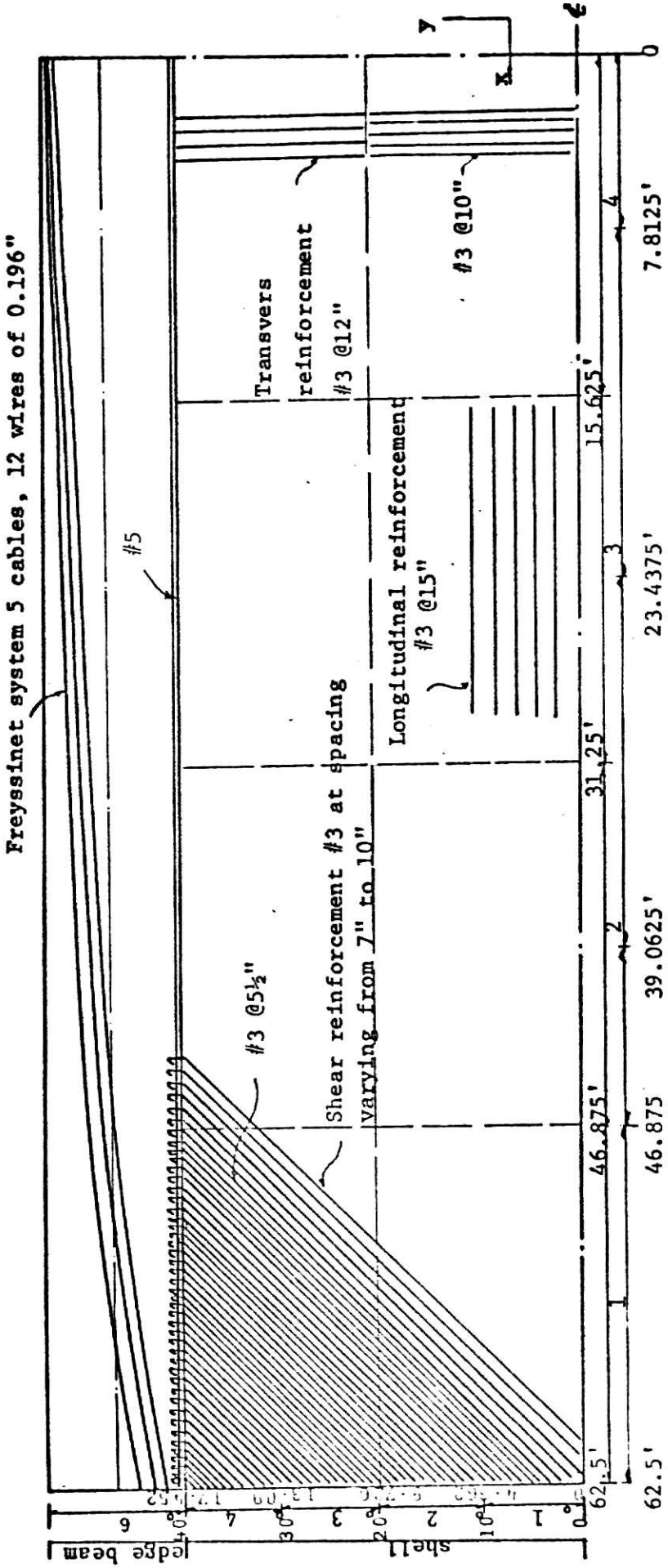

Fig. 18 Cables and Reinforcement Placement of P/C Shell with Edge Beams

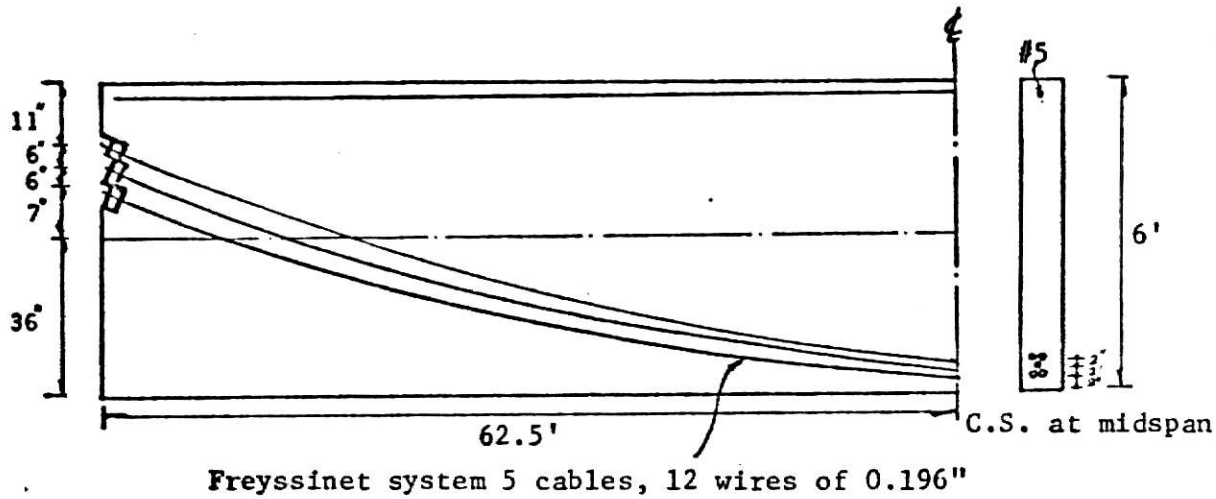

Freyssinet system 5 cables, 12 wires of 0.196"

Fig. 19 Prestressing Cables in the Edge Beam of P/C Shell

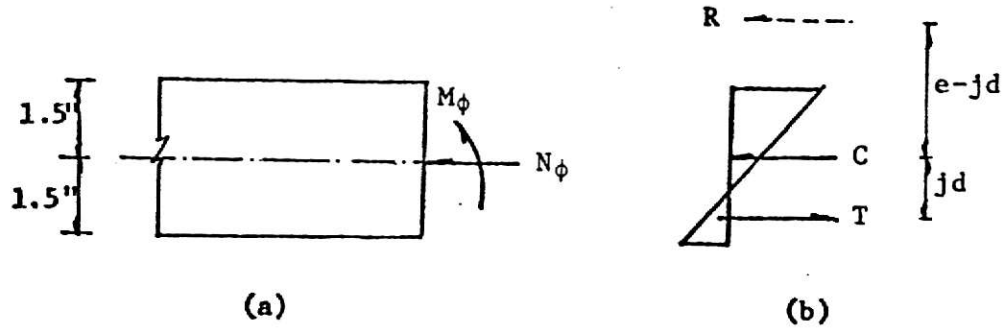

Fig. 20 Shell Section with Transverse Moment and Thrust

ANALYSIS AND DESIGN P/C CYLINDRICAL SHELLS

by

WAIN-LAI KUO

Diploma, Taipei Institute of Technology, 1968

AN ABSTRACT OF A MASTER'S REPORT

submitted in partial fulfillment of the

requirement for the degree

MASTER OF SCIENCE

Department of Civil Engineering

KANSAS STATE UNIVERSITY

Manhattan, Kansas

1976

ABSTRACT

This report presents the analysis and design of P/C cylindrical shells with and without edge beams. These shells are of the same span, redius and semicentral angle. The analysis of the shell with edge beams is based on membrane theory and bending theory and the shell without edge beam is based on the load balancing method and beam theory.

Comparisons were made between the two designs in terms of stress distributions. From these analyses and designs, the following conclusions were reached:

(1) Beam theory is much easier and simpler to apply than bending theory.

(2) It is much easier to layout the cables on the edge beam than along the shell surface.

(3) The P/C shell without edge beams needs more cables and reinforcement but less concrete, than the P/C shell with edge beams.